Quasi-periodic oscillations in GX 17+2

Penninx, W.; Lewin, W.H.G.; Mitsuda, K.; van der Klis, M.; van Paradijs, J.; Zilstra, A.A.

DOI
10.1093/mnras/243.1.114
Publication date
1990

Published in
Monthly Notices of the Royal Astronomical Society

Mon. Not. R. astr. Soc. (1990) **243**, 114–125

Quasi-periodic oscillations in GX 17 + 2

W. Penninx,[1,2] W. H. G. Lewin,[1] K. Mitsuda,[3] M. van der Klis,[2,4] J. van Paradijs[2] and A. A. Zijlstra[5]

[1] *Massachusetts Institute of Technology, Center for Space Research, Room 37–627, Cambridge, MA 02139, U.S.A.*
[2] *Astronomical Institute 'Anton Pannekoek', University of Amsterdam, Roetersstraat 15, 1018 WB Amsterdam, The Netherlands* and *Center for High-energy Astrophysics, NIKHEF-H, Kruislaan 409, 1098 SJ Amsterdam, The Netherlands*
[3] *Institute of Space and Astronautical Science, 3-1-1 Yoshinodai, Sagamihara-shi, Kanagawa-ken, 229 Japan*
[4] EXOSAT *Observatory, Astrophysics Division, Space Science Department of the European Space Agency, Postbus 299, 2200 AG Noordwijk, The Netherlands*
[5] *Kapteyn Laboratorium, PO Box 800, 9700 AV Groningen, The Netherlands*

Accepted 1989 August 30. Received 1989 June 28; in original form 1989 February 1

SUMMARY

We have made X-ray observations of GX 17 + 2 with the *Ginga* Observatory and observed the source in three spectral states: the flaring branch, the normal branch and the horizontal branch. Quasi-periodic oscillations (QPO) were observed in all three branches. In the horizontal-branch state the power spectra show low-frequency noise (LFN), with rms strength between 2.8 and 4.5 per cent, and two QPO peaks, with rms strengths between ~ 1.5 and ~ 3.5 per cent. The latter are most likely to be a first and second harmonic since the ratio of their frequencies, which both vary with intensity, is 2.04 ± 0.06. The centroid frequency of the first harmonic varies from ~ 18 to 30 Hz. The FWHM of the second-harmonic QPO peak is substantially higher than that of the first harmonic. In the normal branch, QPO was observed (rms strength between 1.4 and 2.9 per cent), with a frequency of ~ 7 Hz, independent of the source intensity. When GX 17 + 2 was in the flaring branch state, it showed QPO (rms strength 2.8 to 4.1 per cent) whose frequency, which varied between ~ 7 and ~ 18 Hz, was positively correlated with the X-ray intensity. Simultaneously with these 7–18 Hz QPO we also observed a high-frequency peak in the power spectrum at ~ 120 Hz (rms variation ~ 2 per cent). No LFN was observed in the normal and flaring branches. Very low-frequency noise (below ~ 0.03 Hz) was present in all three spectral branches. Our results show that GX 17 + 2 is a clear example of the recently defined group of Z-type sources. The continuous variation of the QPO behaviour as GX 17 + 2 moves from the normal to the flaring branch, similar to what has been observed in Sco X-1 (and perhaps Cir X-1), indicates that the normal-branch QPO and the flaring branch QPO are likely one physical phenomenon.

1 INTRODUCTION

The X-ray flux of the bright bulge source GX 17 + 2 (Bradt *et al.* 1971) varies irregularly on time-scales of hours and longer (Forman, Jones & Tananbaum 1976; Ponman 1982b). Possible coherent variability has been reported with periods of 31.8 min (White *et al.* 1976), 1.4 hr (Langmeier *et al.* 1986), 19.5 hr (Hertz & Wood 1986) and 6.4 d (Ponman 1982a). Independent confirmation of any of these periodicities is, in our opinion, required. GX 17 + 2 occasionally emits X-ray bursts (Kahn & Grindlay 1984; Tawara *et al.* 1984; Sztajno *et al.* 1986). Although the relative flux increase in these bursts, above the persistent level, is small and some bursts last very long (up to ~ 5 min), these events are probably bona fide type-1 X-ray bursts (Sztajno *et al.* 1986), possibly ignited in a hydrogen-rich environment (van Paradijs, Penninx & Lewin 1988). GX 17 + 2 is also a source of variable radio emission (Hjellming & Wade 1971; Grindlay & Seaquist 1986; Penninx *et al.* 1988). A 17th magnitude optical star is located inside the radio error box

(Tarenghi & Reina 1972), but this G-type star (Davidsen, Malina & Bowyer 1976) is unlikely to be the companion of the X-ray source (Lewin & van Paradijs 1985).

GX 17+2 is a member of the class of low-mass X-ray binaries (LMXB) that show three branches, connected in a Z-shaped pattern in X-ray colour–colour (and also in hardness–intensity) diagrams, and two different types of QPO (Hasinger & van der Klis 1989). The branches are called horizontal (HB), normal (NB) and flaring (FB) branch. When the spectral state of GX 17+2 corresponded to a location on the normal branch in a spectral-hardness versus intensity diagram, QPO were observed at a frequency of ~7 Hz, which did not vary significantly with source intensity (Stella, Parmar & White 1987; Langmeier, Hasinger & Trümper 1990). In the horizontal-branch spectral state GX 17+2 showed intensity-dependent QPO with frequencies between ~24 and ~28 Hz (Stella *et al.* 1987; Langmeier *et al.* 1989). Thus, the QPO behaviour of GX 17+2 is similar to that of, e.g. GX 5-1 and Cyg X-2 (see Lewin, van Paradijs & van der Klis 1988 and van der Klis 1989b, for reviews on QPO). Langmeier *et al.* (1985) found a broad peak at ~24 Hz, which at the time was interpreted as QPO. The source was then on the horizontal branch (Langmeier *et al.* 1990), but the frequency did not vary with source intensity; also, QPO at ~25 Hz were observed simultaneously (Stella *et al.* 1987; Langmeier *et al.* 1990). The former component in the power spectrum of GX 17+2 is now interpreted as 'peaked' LFN (Hasinger & van der Klis 1989). Similar peaked LFN occurs in Sco X-1 (Hasinger, Middleditch & Priedhorsky 1989a). A flaring branch in GX 17+2 was previously observed with *Copernicus* (White *et al.* 1978), *Einstein* (Garcia 1987) and *EXOSAT* (Hasinger 1988).

We observed GX 17+2 with the X-ray observatory *Ginga*. Part of these observations were simultaneous with radio observations with the Very Large Array synthesis radio telescope. We found that the radio brightness was correlated with the X-ray spectral state (Penninx *et al.* 1988). We report here on the relation of the QPO behaviour of GX 17+2, to the X-ray spectral properties (i.e. spectral branches in X-ray colour–colour diagrams) during these observations. A detailed analysis of the photon energy dependence of the QPO, including a time-lag analysis, will be given in a forthcoming paper (Penninx *et al.* 1990). A study of the X-ray spectrum of GX 17+2, in terms of spectral models, will be presented elsewhere, together with results for other low-mass X-ray binaries. The results of a search for coherent periodic oscillations in these data of GX 17+2, and in *Ginga* data of other sources, will be reported by Vaughan *et al.* (1990).

2 OBSERVATIONS

The observations (see Table 1) were made between 1988 March 28 and April 5 with the Large Area Counter, LAC of *Ginga* (Makino 1987; Turner *et al.* 1989), which has an effective area of ~4000 cm^2. As a result of Earth occultation, high-particle background in the South Atlantic Anomaly and limitations in the on-board data recording capacity, observations could be made continuously for time intervals up to at most ~30 min. The data were accumulated in three different modes (the so-called MPC3, MPC1 and PC modes). In the MPC3 mode we had 12 energy channels (covering the photon energy range ~1–37 keV), and a time resolution of 7.8 ms. In the MPC1 mode we had 48 energy channels, and a time resolution between 0.5 and 2 s. The MPC1 data were not used for the timing analysis. In the PC mode the two halves of the detectors were recorded separately, in two energy channels each. The channel boundaries of one half were 1–2.9 keV (with 1 ms time resolution) and 2.9–12.2 keV (2 ms); those of the other half were 1–7.9 keV (1 ms) and 7.9–12.2 keV (2 ms). The background was measured after the instrument had moved off-source on March 29. The counting rate of the background is typically 50 ct s^{-1}, i.e. much less than the source counting rate (see below).

Table 1. Log of the observations.

Day (1988)	Start time	End time	Usable Observing Time	Observing Mode	Source State**
March 28	14:50	16:50	0:40	MPC-1*	Apex
March 28	16:50	21:50	1:30	MPC-3	FB
March 28	21:50	23:30	0:45	PC	FB
March 28	23:30	23:40	0:10	MPC-1*	FB
March 29	15:00	16:55	0:20	MPC-1*	NB
March 29	16:55	18:30	0:30	MPC-3	NB
March 31	15:25	17:00	0:20	MPC-3	NB
April 1 (A)	15:25	15:35	0:10	MPC-3	FB
April 1 (B)	15:55	16:10	0:15	MPC-3	Apex + FB
April 1 (C)	16:55	17:20	0:25	MPC-3	NB
April 1 (D)	17:25	17:50	0:25	MPC-3	NB
April 1 (E)	18:30	19:00	0:30	MPC-3	NB
April 1 (F)	19:10	19:30	0:20	MPC-3	NB
April 1 (G)	20:10	20:30	0:20	MPC-3	FB
April 1	20:30	22:15	0:30	PC	FB
April 4	14:10	19:10	1:20	MPC-3	HB
April 4	19:10	20:50	0:40	PC	HB
April 5	12:30	17:30	0:50	MPC-3	HB
April 5	17:30	19:10	0:45	PC	HB

*Not used in timing analysis.
**FB = flaring branch, NB = normal branch, HB = horizontal branch.

3 ANALYSIS AND RESULTS

The X-ray data were corrected for spacecraft attitude, background, and dead-time (for a discussion of the dead-time correction we refer to Mitsuda & Dotani 1989a). The attitude of the spacecraft, which is stable to within ~10 arcsec on time-scales of less than a minute, was determined to an accuracy of ~3 arcmin. This introduced a ~5 per cent uncertainty in the source flux. In Fig. 1 we show the time variation of the source intensity, I (count rate between 1 and 37 keV for MPC modes and 1–12 keV for PC mode), and a spectral hardness (expressed as a ratio of the count rates in two energy channels: 7.0–11.6/2.3–7.0 keV for MPC modes and 7.9–12.2/2.9–7.9 keV for PC mode). The count rate varied between ~5000 and 12 000 s^{-1}, corresponding to a flux between $\sim 1.4\times10^{-8}$ and $\sim 3.4\times10^{-8}$ erg cm^{-2} s^{-1} (1–20 keV), which is within the range observed earlier from GX 17+2 (Bradt *et al.* 1971; Forman *et al.* 1978; McHardy

et al. 1981; Sztajno *et al.* 1986). Fig. 2 shows 'hardness–intensity diagrams', in which hardness ratio is plotted versus *I*. Fig. 3 shows 'X-ray colour–colour diagrams' in which a soft hardness ratio is plotted on the horizontal axis versus a hard hardness ratio on the vertical axis; these ratios are indicators of the spectral slope in the low- and high-energy parts of the spectrum, respectively. It can be seen that the detailed shape of the spectral branches in these diagrams depends on the particular choice of photon energy bands which define the intensity and the hardness ratios.

In Figs 2 and 3 we have indicated the normal branch (NB), the horizontal branch (HB), and the flaring branch (FB). These spectral branches, seen previously in *EXOSAT* data from Cyg X-2, Sco X-1, GX 5-1, GX 17+2, GX 349+2 and GX 340+0, characterize the 'Z sources' (Hasinger *et al.* 1989a; Hasinger & van der Klis 1989). During our observations we encountered GX 17+2 in all three spectral states. The horizontal branch is vertical in Fig. 3; although there is some dependence on the choice of the energy channels, a steep horizontal branch appears to be the normal state of affairs for GX 17+2 (compare e.g. Langmeier *et al.* 1990). Similar vertical HB's have been seen in Sco X-1 by Hasinger *et al.* (1989a). The identification with the horizontal branch is fairly certain from the fact that in this branch the frequency of the QPO (which ranged from ~18 to ~30 Hz) was intensity dependent (see below) in a way similar to that in the horizontal branch observed for other sources (for a review see Lewin *et al.* 1988). The spectral behaviour of GX 17+2 is better defined in the colour–colour diagram (Fig. 3) than in the hardness–intensity diagram (Fig. 2). As indicated above, the accuracy of the spacecraft attitude is limited. However, the stability on shorter time-scales (~1 hr) is rather good (≲1 per cent in count rate), and an intensity variation on April 4 of ~5 per cent was noticeable without any change in hardness ratio. This may be similar to what was found for Cyg X-2 on longer time-scales (Hasinger 1987a).

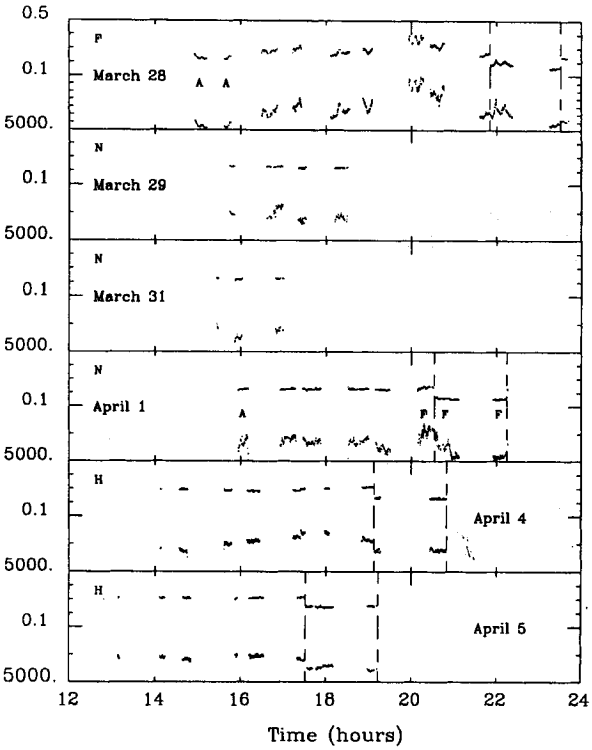

Figure 1. X-ray intensity (1–37 keV) and the spectral hardness ratio (7.0–11.6/2.3–7.0 keV) of GX 17+2 as a function of time. Top trace in each panel corresponds to spectral hardness, bottom trace to intensity. The spectral hardness scale in each panel runs from 0.1–0.5; the intensity scale from 5000–12 000 c s^{-1} in the top panel and from 5000–7000 c s^{-1} in the other panels. Consecutive tic marks represent changes of 1000 c s^{-1} (intensity) and 0.1 (hardness ratio). During the last part of the observations made on March 28 and April 1, 4 and 5, respectively, GX 17+2 was observed with the PC-mode, with limited energy resolution (X-ray lightcurves: 1–12.2 keV; spectral hardness ratio: 7.9–12.2/2.9–7.9 keV). These intervals have been indicated by vertical dashed lines. GX 17+2 was observed in all three known spectral branches (see text and Figs 2 and 3). The spectral branches are indicated: F, N and H stand for flaring, normal and horizontal branch, respectively; the As (March 28 and April 1) indicate the times that the source was near the transition (apex) of the normal and flaring branch (see Figs 2 and 3).

We have estimated the power spectra of the intensity variations by calculating the Fourier amplitudes via a Fast Fourier Transform algorithm. Detector dead-time effects will cause the intensity distribution due to counting noise to deviate slightly from a purely Poissonian distribution, and the associated white-noise power to be slightly lower; these effects are taken into account by subtracting the white-noise level from the power spectra (for details see Lewin *et al.* 1988; van der Klis 1989a; Mitsuda & Dotani 1989a).

The power spectra were calculated for individual data blocks, with a duration of 16 s. The Nyquist frequencies were 64 and 256 Hz, for the MPC-3 and PC-mode (see above), respectively. Four consecutive power spectra were averaged (i.e. over 64 s). In order to extend the frequency range to very low frequencies, we repeated this procedure after rebinning the data by a factor of 4 (MPC3 data) and 16 (PC data); the lowest frequency in these power spectra was 4×10^{-3} Hz.

From an inspection of colour-coded displays of power spectra versus time (see van der Klis *et al.* 1985), we noticed that QPO occurred in all spectral states. Examples of power spectra, as observed in each of these three spectral branches, are shown in Fig. 4. In these power spectra very low-frequency noise (VLFN; see van der Klis *et al.* 1987) is present in all three spectral branches [see Table 2, not visible in the Fig. 4c (HB) due to the limited frequency range that is plotted]. In the horizontal branch the power spectrum also contains an LFN component. This LFN component is absent in the normal and flaring branches. In the power spectra based on PC data, which have a sufficiently high time-resolution (these data cover the horizontal and flaring branches, see Table 1), high-frequency noise (HFN) is present, up to frequencies in excess of 10^2 Hz.

Since the spectral behaviour of GX 17+2 is more well defined in the colour–colour diagram than in the hardness–intensity diagram (see above), we selected the data according to spectral hardness. Because the channel settings were different in the PC and MPC-3 modes, the hardness ratio cannot be defined in the same way for these two sets of data. The hardness ratio for the MPC3 data is defined as the count rate ratio 7.0–11.6/2.3–7.0 keV, for the PC-data as the ratio 7.9–12.2/2.9–7.9 keV (see vertical axes of Fig. 3b and

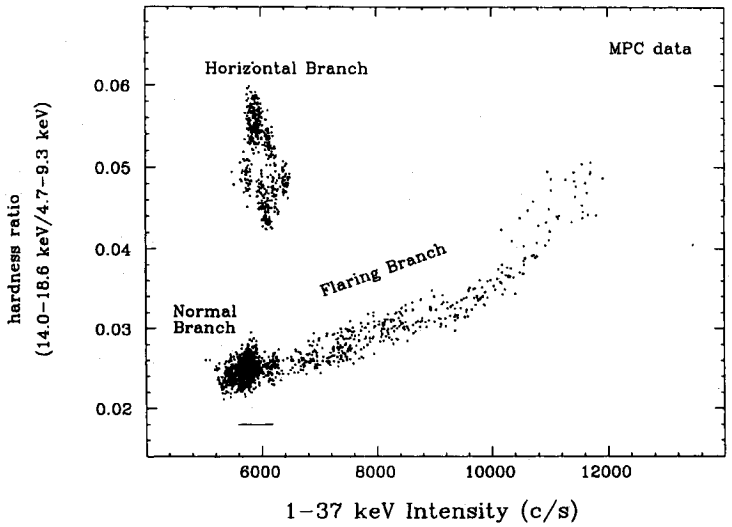

Figure 2. (a) Spectral hardness (14.0–18.6/4.7–9.3 keV)–intensity (1–37 keV) diagram of MPC data (MPC-1 and MPC-3). Each point is a 32-s average. The spectral branches are indicated: flaring branch, normal branch and horizontal branch. The horizontal bar indicates the range in count rate where flaring-branch QPO are found (7–20 Hz).

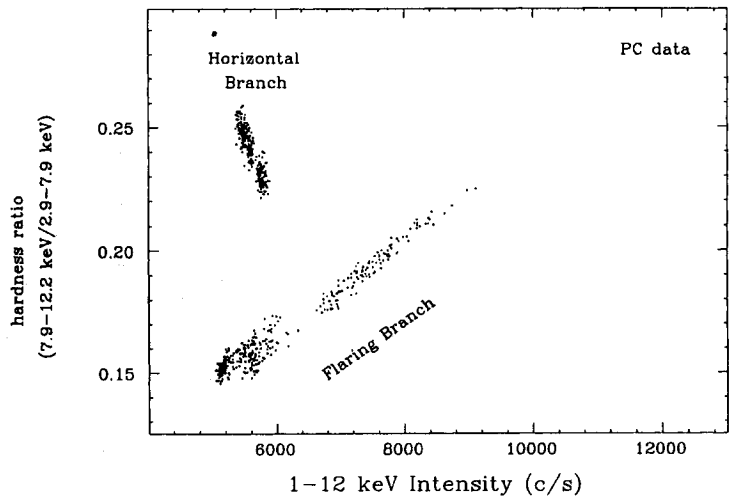

Figure 2. (b) Same as Fig. 2(a) for the PC-data, Spectral hardness (7.9–12.2/2.9–7.9 keV) versus intensity (1–12.2 keV). Each point is a 32-s average.

c, respectively). The choices of the specific values of these hardness ratios were a compromise between the requirements of good statistics (low energy range) and a sufficient range in hardness ratio (high energy range). We fitted the average power spectra, selected for each day separately according to these hardness ratios, with different fit functions described below.

3.1 Flaring and normal branch

For the normal-branch and flaring branch data the power spectrum was fitted with a function that included a power law $\nu^{-\Gamma}$ for the very low-frequency noise component (VLFN; see e.g. van der Klis *et al.* 1987), and a Lorentzian for the QPO peak. No separate component was used to describe a low-frequency noise component or a high-frequency noise component. In Table 2 we list for these data sets the QPO centroid frequency, the FWHM of the QPO peak, the values of Γ for the VLFN, and the excess power (rms variation) of the QPO, and the VLFN (for details see caption of Table 2). In the normal branch the frequency of the QPO does not vary much with spectral hardness. The average frequency equals 7.1 ± 0.3 Hz (the uncertainty is one standard deviation of the distribution of the individual values). This value, which is consistent with the range 6.67–7.8 Hz, found by Stella *et al.* (1987) for GX 17 + 2, is similar to the values found for other QPO sources in the normal-branch spectral state (Hasinger 1987b; van der Klis 1989b).

QPO were present on the lower part of the flaring branch, with frequencies between ~7 and ~20 Hz. The QPO frequency was near 7 Hz at the apex (connection between the normal and flaring branch), and increased with hardness ratio (and source intensity; see Table 2). The range in count rates where QPO are found on the flaring branch is indicated in Fig. 2(a) with a horizontal bar. At larger hardness ratios (and intensities) no well-defined QPO peaks were found. However, excess power was present, but spread over a large frequency range. When fitted with a Lorentzian, the FWHM of the QPO peak was often much larger than the centroid frequency (see Table 2, note c). As the source moved up the flaring branch, the rms excess power between 0.5 and 10 Hz decreased, while that at lower frequencies (0.004–0.1 Hz) increased. This 'leakage' of QPO power over a very broad-frequency range, as the source moves up the flaring branch, is similar to what has been reported in Sco X-1 (Middleditch & Priedhorsky 1986). It should be noted that in Sco X-1 excess power at high frequencies, up to $\sim 10^2$ Hz, has also been observed when it was in other spectral branches (Hasinger *et al.* 1989a), and the same is the case in some other sources as well (Hasinger & van der Klis 1989).

We show in Fig. 5 the average power spectrum of the April 1 PC-data (flaring branch). In this power spectrum the intensity-dependent QPO in the frequency range 6–30 Hz are

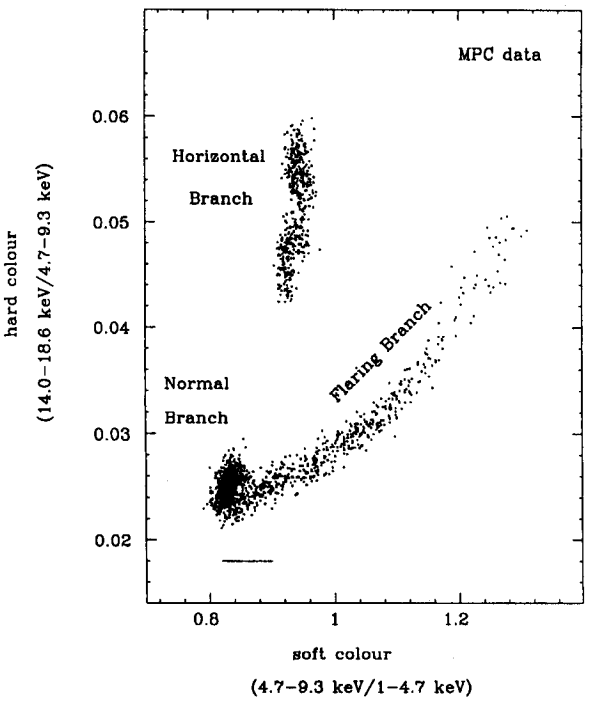

Figure 3. (a) X-ray 'Colour–colour' diagram of all MPC data (MPC-1 and MPC-3). Each point is a 32-s average. The ordinate and the abscissa show the spectral hardness ratios (14.0–18.6/4.7–9.3 keV) and (4.7–9.3/1–4.7 keV), respectively. The spectral branches are indicated: flaring branch, normal branch and horizontal branch. Ironically the horizontal branch is vertical in this diagram; the identification, however, leaves little doubt (see text and Fig. 2). The horizontal bar indicates the range where QPO is found on the flaring branch (7–20 Hz).

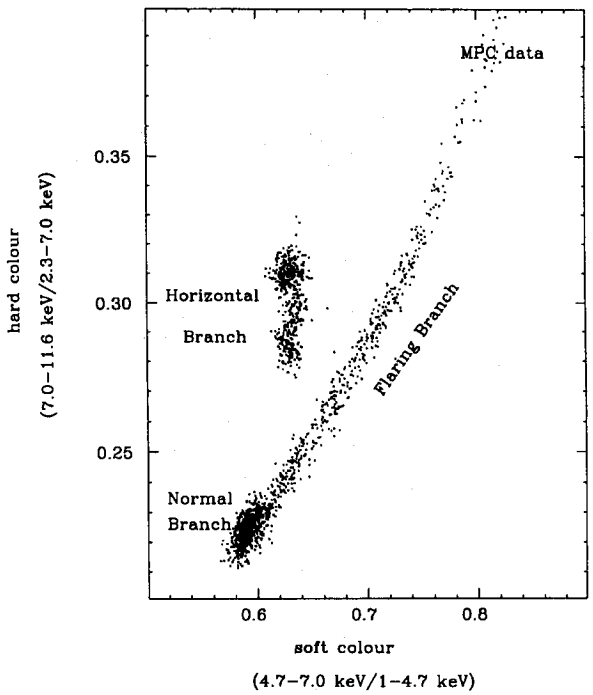

Figure 3. (b) Same as Fig. 3(a) (MPC-1 and MPC-3 data). The ordinate and the abscissa show the spectral hardness ratios (7.0–11.6/2.3–7.0 keV) and (4.7–7.0/1–4.7 keV), respectively. The hardness ratio on the vertical axis was used for selection in the timing analysis (MPC-3 data).

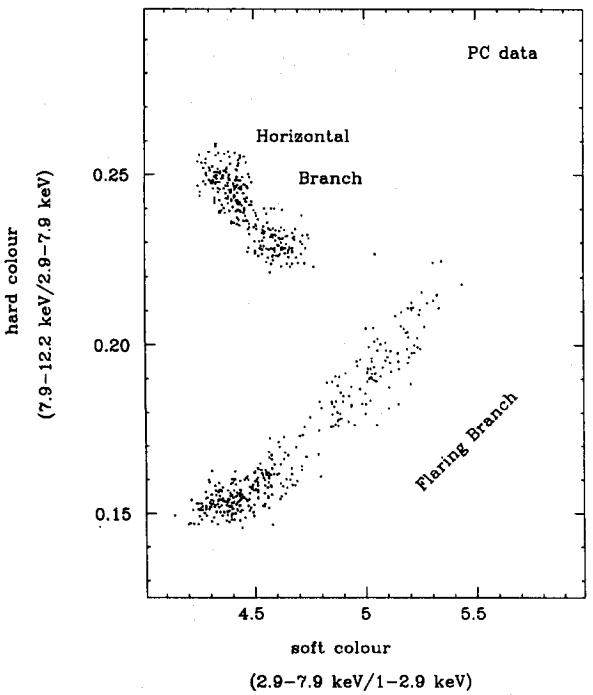

Figure 3. (c) Same as Fig. 3a for PC-data. The ordinate and the abscissa show the spectral hardness ratios (7.9–12.2/2.9–7.9 keV) and (2.9–7.9/1–2.9 keV), respectively. The hardness ratio on the vertical axis was used for selection in the timing analysis (PC-data).

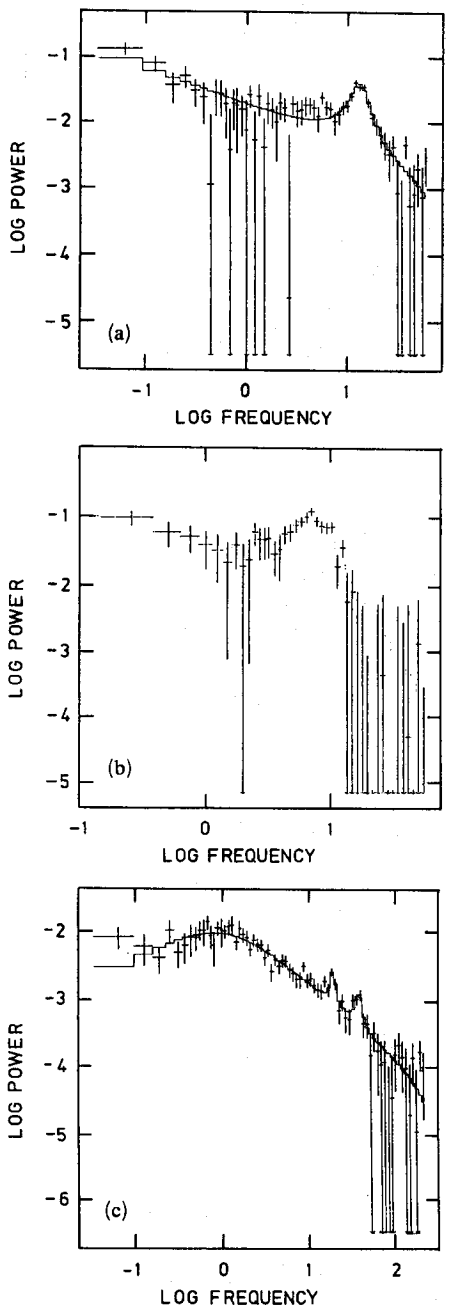

Figure 4. Examples of power spectra on the (a) flaring branch (PC-data, set III of April 1), (b) the normal branch (MPC-3 data, March 29) and (c) the horizontal branch (PC-data, April 5). Notice the first and second harmonic QPO on the horizontal branch.

smeared out, and appear as a very broad bump. A very high-frequency peak is present near ~120 Hz with an rms variation of ~2 per cent (see Table 3). The data are not of sufficient statistical quality to study the dependence of this very high-frequency peak on source intensity (or spectral hardness). Very high-frequency peaks with frequencies in excess of $\sim 10^2$ Hz have previously only been reported from Cir X-1 (Tennant 1987). Hasinger & van der Klis (1989) have suggested that such a broad very high-frequency peak may be a manifestation of HFN, similar to the presence of peaked LFN components observed in the power spectra of some sources. We do not expect the peak reported here to belong to the HB or FB/NB QPO.

3.2 Horizontal branch

In all of the horizontal-branch data sets for which the statistical significance is sufficient, we find two QPO peaks in the power spectrum. The ratio of their centroid frequencies equals 2.04 ± 0.06 (one standard deviation). Within the accuracy of the measurements, this ratio does not depend on the centroid QPO frequency, which varies from ~18 to ~30 Hz (first harmonic). This result indicates that these two peaks are the first and second harmonics of the QPO. The FWHM of the second-harmonic QPO peak is larger than that of the first harmonic by a factor of 2.02 ± 0.46 (90 per cent error-bar), inconsistent with pure lifetime broadening and consistent with broadening due to frequency shifts. The horizontal-branch data also contain a strong (peaked) LFN component. The power spectra for these data (0.06 to 64 or 256 Hz) were fitted to a Lorentzian with a second harmonic at precisely double the frequency of the first harmonic, and a function $[A\nu^{-\Gamma} + B\nu^{\Psi}]^{-1}$ to describe (rather arbitrarily) the LFN component. Functions (such as an exponential, Lorentzian centered at 0 Hz, or an exponentially cut-off power law) which were used previously to describe the LFN, gave bad fits; also the LFN observed with *Ginga* in GX 5-1 (HB state) could not be fitted with these conventional shapes (Mitsuda & Dotani 1989b). No VLFN component was necessary to describe these power spectra in the 0.06–64 Hz range. The results of our functional fits to the power spectra are listed in Table 2.

In the horizontal branch the QPO frequency shows a variation as a function of spectral hardness (see Table 2). The range of frequency observed is ~18 to ~30 Hz, which includes and extends the range observed previously for GX 17+2 (Stella *et al.* 1987), and is similar to the frequency intervals observed for horizontal-branch QPO in other sources. Since the location of the horizontal branch in the hardness–intensity diagram does not appear to be unique (see above), it is not possible to transform this relation between spectral hardness and QPO frequency into a frequency–intensity relation.

3.3 Energy dependence

We studied the energy dependence of the QPO, by fitting the power spectra of the MPC-3 data in seven broad energy channels. We found no evidence for differences in centroid frequency and FWHM of the QPO peaks at different photon energies. To determine the rms variation of the QPO as a function of photon energy, the centroid frequency and FWHM were fixed at the values found for the combined data (1–37 keV). To increase the statistics of the energy-selected data on the horizontal and flaring branches the frequency axes of the individual power spectra were rescaled (by a multiplicative factor) such that the QPO peaks fall on top of each other. The QPO rms–energy spectra are presented in Table 4, and examples for the three branches are given in Fig. 6.

1990MNRAS.243..114P

Table 2. (a) Results of the power spectral analysis (1988 March 28–April 1; flaring and normal branch).

Set		HR	ν_{QPO}	FWHM	Γ	A_{QPO}	rms 0.5–10 Hz	rms 0.004–0.1 Hz	rms 64–256 Hz	χ^2
			(Hz)	(Hz)		%	(%)	(%)	(%)	per dof
(1)	(2)	(3)	(4)	(5)	(6)	(7)	(8)	(9)	(10)	(11)
March 28 - MPC3 Data[a] - Flaring Branch										
I	28	0.0	8.6±5.4[c]	22±15[c]	1.90±0.53	2.6±0.6	1.21±0.16	1.24±0.11 (2)		0.74
II	36	0.25	6.5±3.4[c]	10±11[c]	1.78±0.79	1.6±0.6	1.08±0.16	1.24±0.11 (2)		0.74
III	45	0.26	4.5±1.6	9±5[c]	2.11±0.89	2.0±0.4	1.38±0.10	1.11±0.15 (1)		0.59
IV	24	0.27	5.0±3.5[c]	16±8[c]	2.36±0.29	2.5±0.6	1.49±0.12	2.64±0.17 (3)		0.77
V	33	0.28	9.4±2.3	4.9±6.8	1.69±0.46	1.2±0.5	0.88±0.16	1.47±0.16 (1)		0.81
VI	44	0.29	4.9±1.4[c]	140±1.6[c]	1.92±0.56	2.3±0.7	0.99±0.11	2.07±0.16 (1)		1.13
VII	28	0.30	2.1±1.2[c]	111±17[c]	1.53±0.65	0.6±0.8	0.46±0.13	2.50±0.39 (3)		0.84
Γ_{VLFN} = 1.88 ± 0.11 (0.004-0.1 Hz)										
March 28 - PC Data[a] - Flaring Branch										
I	4	0.0	12.6±0.5	2.1±1.6	0.42±0.34	3.1±0.7	2.31±0.32		3.21±1.14	0.69
II	36	0.15	14.0±0.3	4.2±1.0	0.45±0.09	3.2±0.3	1.91±0.11	1.07±0.11 (3)	2.83±0.39	0.80
II	12	0.16	16.2±1.8	11.7±5.3	1.74±1.24	3.7±0.5	1.67±0.22		0.76±2.43	0.66
IV	20	0.17	6.7±1.6[c]	8.3±5.8[c]	0.59±0.29	2.5±0.8	1.88±0.13		1.71±0.72	1.03
V	28	0.18	5.5±0.8	2.5±2.6	0.40±0.14	1.2±0.5	1.50±0.12	1.39±0.16 (2)	2.36±0.41	1.14
VI	44	0.19	7.2±2.4[c]	15.6±7.1[c]	1.87±0.61	2.7±0.5	1.40±0.10	1.85±0.34 (3)	1.30±0.56	0.96
VII	12	0.20	13.7±4.4[c]	14±13[c]	2.58±1.19	2.2±0.8	0.94±0.27	2.00±0.15 (2)	1.26±1.11	0.60
VIII	16	0.21	6.9±11[c]	34±28[c]	2.11±0.47	3.1±1.2	1.27±0.17		2.01±0.55	0.89
Γ_{VLFN} = 1.99 ± 0.02 (0.004-0.1 Hz)										
March 29 - MPC3 Data[a] - Normal Branch										
I	40	0.215	7.7±0.5	5.0±1.6	0.97±0.38	2.7±0.4	2.29±0.09	0.98±0.09 (2)		1.00
II	52	0.22	7.1±0.4	5.9±1.2	1.84±0.40	2.9±0.2	2.24±0.08	0.63±0.12 (3)		1.02
Γ_{VLFN} = 1.43 ± 0.19 (0.004-0.1 Hz)										
March 31 - MPC3 Data[a] - Normal Branch										
I	20	0.215	6.7±0.2	1.4±0.7	2.18±2.62	2.0±0.3	1.94±0.17	0.64±0.17 (2)		0.77
II	44	0.22	7.0±0.4	1.8±1.0	1.42±1.02	1.4±0.3	1.36±0.14	0.90±0.16 (1)		1.01
Γ_{VLFN} = 0.65 ± 0.62 (0.004-0.1 Hz)										
April 1 - MPC3 Data[a] - Normal-Flaring Branch										
A[b]	28		14.1±0.4	3.7±1.2	0.64±0.19	3.5±0.4	2.09±0.15			0.77
B[b]	56		12.7±0.5	6.8±1.9	0.49±0.12	3.7±0.5	2.55±0.09	1.17±0.10 (2)		1.19
C[b]	72		6.7±0.1[d]	0.8±0.8[d]	0.20±0.10	1.2±0.3	2.06±0.09	0.67±0.08 (1)		0.70
D[b]	96		7.2±0.7	1.7±0.2	0.48±0.14	0.9±0.4	1.48±0.10	0.74±0.09 (1)		0.92
E[b]	89		6.9±0.4[d]	0.7±0.8[d]	0.64±0.17	2.6±0.3	1.43±0.11			0.49
F[b]	80		7.2±0.4	4.0±1.2	0.64±0.17	2.6±0.3	2.52±0.08	0.94±0.07 (3)		1.18
G[b]	68		18.4±1.5	8.1±5.1	0.51±0.15	2.1±0.6	1.61±0.11	1.64±0.20 (1)		1.47
Γ_{VLFN} = 1.56 ± 0.12 (0.004-0.1 Hz)										
April 1 - PC Data[a] - Flaring Branch										
I	36	0.15	6.8±1.1[c]	9.5±4.1[c]	0.77±0.27	3.6±0.8	2.6±0.1	1.04±0.12 (3)	1.87±0.64	0.89
II	52	0.1525	8.9±0.7[c]	10.1±2.4[c]	0.59±0.14	4.1±0.4	2.7±0.1	0.71±0.08 (2)	2.12±0.46	0.87
III	24	0.155	16.0±1.2	9.1±4.3	0.74±0.38	3.2±0.6	1.7±0.2	2.07±0.15 (1)	1.42±0.89	0.86
IV	28	0.1575	17.0±9.1	6.5±2.8	0.53±0.16	2.9±0.5	1.7±0.1	0.89±0.12 (2)	2.49±0.51	1.02
V	20	0.16	18.6±1.1	6.5±3.4	0.54±0.16	2.8±0.5	1.8±0.2		1.56±0.96	1.01
Γ_{VLFN} = 1.99 ± 0.02 (0.004-0.1 Hz)										

[a]MPC-3: energy range 1–37 keV, time resolution 8 ms. FFT (0.06–64 Hz) contain 16 s of data; FFT (0.004–16 Hz) contain 256 s of data. PC: energy range 1–12.2 keV, time resolution 2 ms. FFT (0.06–256 Hz) contain 16 s of data; FFT (0.004–16 Hz) contain 256 s of data.
[b]These data sets indicated with letters, are listed in time sequence, they were not selected by hardness ratio. They combine normal-branch and flaring-branch data; a selection by hardness would be meaningless (see Fig. 2).
[c]QPO signature ambiguous; the FWHM of the peak is larger than the centroid frequency.
[d]QPO not meaningful; detection in only one frequency resolution bin.

The data were fitted to a Lorentzian plus power law (see text).
(1) Data sets sorted according to spectral hardness ratio (column 3), however, see footnote b.
(2) Number of 16-s intervals available.
(3) Hardness ratio 7.0–11.6/2.3–7.0 keV for MPC3 data, 7.9–12.2/2.9–7.9 keV for PC data. The number listed is the lower boundary for that set, the number in the next row is the upper boundary; the last set has a lower boundary only.
(4) Centroid QPO frequency (in Hz).
(5) Full width at half maximum (in Hz) of QPO peak.

[*Continued opposite*]

Table 2. (b) Results of the power spectral analysis (1988 April 4–5; horizontal branch).

Set		HR	ν_{QPO}	FWHM$_1$	FWHM$_1$	Γ_1	Γ_2	A_{QPO_1}	A_{QPO_2}	rms 0.5–10 Hz	rms 0.004–0.1 Hz	rms 64–256 Hz	χ^2
			(Hz)	(Hz)	(Hz)			(%)	(%)	(%)	(%)	(%)	per dof
(1)	(2)	(3)	(4)	(5)	(6)	(7)	(8)	(9)	(10)	(11)	(12)	(13)	(14)
					April 4 - MPC3 Data[a] - Horizontal Branch								
I	60	0.28	27.1±0.1	23±25	0.1±0.5[d]	0.02±0.14	2.49±0.82	2.5±1.2	1.3±0.4	0.36±0.08 (3)	2.80±0.07		0.97
II	57	0.285	31.2±0.8	4.0±0.8	7.5±14	0.45±0.19	1.48±0.10	2.0±0.3	1.6±1.2	0.43±0.07 (1)	2.98±0.07		0.78
III	36	0.29	29.0±1.3	2.8±2.9	6.8±18	0.40±0.29	1.08±0.31	1.7±0.6	1.8±1.6	0.48±0.08 (2)	3.29±0.09		1.14
IV	40	0.295	30.0±1.1	11.9±1.8	5.6±18	0.40±0.14	1.33±0.09	1.5±0.3	1.6±1.2	0.45±0.07 (2)	3.17±0.07		0.93
V	20	0.30	24.4±0.6	30.3±9.3	15.1±2.8	0.60±0.10	1.79±0.05	2.9±3.4	1.2±0.3		3.14±0.09		1.49
VI	28	0.305	25.6±0.9	4.3±5.4	6.5±5.5	0.53±0.31	1.25±0.27	1.7±0.8	2.5±0.7	0.64±0.07 (2)	3.43±0.08		0.62
Γ_{VLFN} = 0.12 ± 0.42 (0.004-0.1 Hz)													
					April 4 - PC Data[a] - Horizontal Branch								
I	25	0.225	27.1±0.7	3.1±2.0	17.0±17	0.22±0.22	1.33±0.29	2.2±0.2	2.4±0.4	0.63±0.04 (1)	3.71±0.04	2.80±0.22	0.77
II	40	0.2275	25.8±0.5	1.7±1.7	11.8±11	0.24±0.15	1.22±0.17	2.1±0.4	2.1±0.8	0.63±0.08 (2)	3.69±0.07	2.68±0.38	1.01
III	28	0.23	26.5±0.8	4.8±2.6	12.9±8.6	0.61±0.27	1.18±0.18	2.4±0.5	2.8±0.7	0.52±0.06 (2)	3.77±0.08	3.35±3.64	0.93
IV	12	0.2325	25.0±1.2	5.3±4.6	6.9±26	0.51±0.45	1.19±0.30	2.6±0.8	1.4±1.6		3.81±0.13	2.86±0.68	0.84
V	4	0.235	26.0±1.5	16.2±22	6.1±6.1	0.78±1.01	1.41±0.60	3.7±2.2	3.2±1.1		3.41±0.25	1.77±2.01	0.97
Γ_{VLFN} = 1.14 ± 0.20 (0.004-0.1 Hz)													
					April 5 - MPC3 Data[a] - Horizontal Branch								
I	16	0.300	21.7±0.9	4.1±4.0	7.0±7.1	0.05±0.25	1.53±0.70	2.3±0.9	2.8±1.0		3.79±0.12		0.70
II	84	0.305	21.5±0.4	5.3±1.8	8.7±3.2	0.15±0.12	1.60±0.26	2.0±0.4	3.0±0.4	0.60±0.04 (6)	3.79±0.05		1.13
III	88	0.310	21.4±0.5	5.2±1.9	12.5±6.5	0.24±0.15	1.40±0.22	2.6±0.4	2.8±0.6	0.80±0.08 (3)	3.87±0.05		1.24
IV	16	0.315	20.4±0.1	10.5±7.7	0.03±0.15[d]	1.34±0.75	1.15±0.30	3.5±1.3	1.8±0.5		4.00±0.12		1.00
Γ_{VLFN} = 0.32 ± 0.18 (0.004-0.1 Hz)													
					April 5 - PC Data[a] - Horizontal Branch								
I	4	0.235	24.7±2.2	10.8±4.8	1.0±4.7[d]	0.05±0.15	0.80±0.05	3.2±0.5	2.2±0.4		4.15±0.22	3.23±1.14	1.58
II	16	0.24	22.5±0.4	5.2±2.7	2.3±8.1	0.82±0.47	1.00±0.14	3.0±0.6	2.0±0.8	0.64±0.06 (4)	4.21±0.10	3.60±0.48	0.90
III	36	0.2425	22.4±0.4	4.4±2.0	6.4±4.4	0.46±0.22	1.14±0.13	2.6±0.4	2.6±0.5		4.11±0.07	2.74±0.40	1.04
IV	16	0.245	21.4±0.5	4.9±2.7	6.3±3.2	0.24±0.26	1.14±0.13	3.1±0.6	3.1±0.6	0.60±0.07 (2)	4.19±0.11	2.45±0.71	0.99
V	36	0.2475	20.5±0.3	3.6±1.2	8.5±3.3	0.27±0.24	1.25±0.17	3.0±0.4	3.4±0.5	0.69±0.04 (1)	4.23±0.07	2.86±0.40	1.24
VI	16	0.25	20.4±0.4	2.4±1.6	6.0±5.8	0.62±0.35	1.07±0.13	2.4±0.5	2.6±0.8	0.73±0.04 (1)	4.26±0.11	3.69±0.57	0.87
VII	29	0.2525	19.5±0.4	3.1±1.7	8.2±3.9	0.58±0.23	1.01±0.09	2.4±0.4	3.0±0.6	0.65±0.05 (1)	4.51±0.08	4.30±0.30	1.26
Γ_{VLFN} = 0.47 ± 0.20 (0.004-0.1 Hz)													

The data were fitted to a Lorentzian with a second harmonic at precisely double the frequency of the first harmonic, and a combination of two power laws with indices Γ_1 and Γ_2 (see text).

(1) Data sets sorted according to spectral hardness ratio (column 3).
(2) Number of 16-s intervals available.
(3) Hardness ratio 7.0–11.6/2.3–7.0 keV for MPC3 data, 7.9–12.2/2.9–7.9 keV for PC data. The number listed is the lower boundary for that set, the number in the next row is the upper boundary; the last set has a lower boundary only.
(4) Centroid QPO frequency (in Hz).
(5) Full width at half maximum (in Hz) of QPO peak.
(6) Full width at half maximum (in Hz) of the second harmonic QPO peak.
(7) Best value of the power-law index Γ_1 (see text).
(8) Best value of the power-law index Γ_2 (see text).
(9) rms variation of the QPO; integration of best fit Lorentzian.
(10) rms variation of the second harmonic of the QPO; integration of best fit Lorentzian.
(11) rms variation between 0.5–10 Hz (integration of actual data points).
(12) rms variation between 0.004–0.1 Hz (integration of data points); the number of 256-s available data sets is given in brackets. Combining the available data of all sets, the best fit power-law index Γ_{VLFN}, as determined between 0.004 and 0.1 Hz, is given separately on the line below the last set.
(13) rms variation between 64–256 Hz (integration of actual data points).
(14) χ^2 per degree of freedom.

---

(6) Best value of VLFN power-law index Γ (see text), as determined between 0.06 and 64 Hz (MPC-3) or 0.06–256 Hz (PC mode).
(7) rms variation of the QPO; integration of best fit Lorentzian.
(8) rms variation between 0.5–10 Hz (integration of actual data points).
(9) rms variation between 0.004–0.1 Hz (integration of data points); the number of 256-s available data sets is given in brackets. Combining the available data of all sets, the best fit power-law index Γ_{VLFN}, as determined between 0.004 and 0.1 Hz, is given separately on the line below the last set.
(10) rms variation between 64–256 Hz (integration of actual data points).
(11) χ^2 per degree of freedom.

Above ~5 keV the QPO energy spectra of all data sets are harder than the total energy spectrum. There is a suggestion that on April 1 (normal and flaring branch) and April 4 and 5 (horizontal branch) the rms values in the lowest energy channel (1–2.3 keV) were larger than in the next energy channel (2.3–4.6 keV). This is similar to what was found for Cyg X-2 (Mitsuda & Dotani 1989a). It is not clear whether this effect is intrinsic to the source; due to the argon escape peak in the detector a considerable fraction of the photons detected below 2.3 keV will actually come from ~4–5 keV. No increase in the rms variation was found below 2.3 keV on March 29 and 31 (NB).

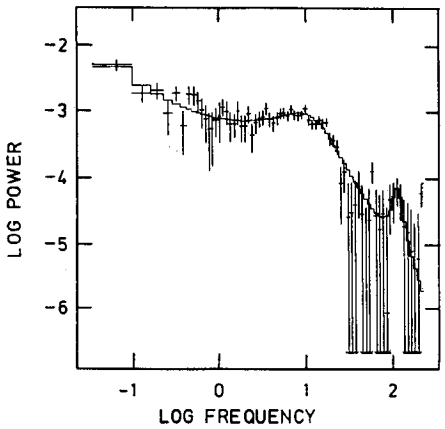

Figure 5. Averaged power spectrum of the flaring branch PC-data on April 1.

Table 3. High-frequency peak on the flaring branch.

	March 28	April 1
Freq (Hz)	127^{+17}_{-7}	123^{+18}_{-14}
FWHM (Hz)	37^{+79}_{-24}	29^{+57}_{-27}
rms mod. (%)	$1.81^{+0.63}_{-0.56}$	$1.63^{+0.85}_{-0.64}$

Errors are 90 per cent confidence intervals (Avni 1976).

4 DISCUSSION

The bright low-mass X-ray binaries (LMXB) have 'family traits' with respect to their spectral behaviour (as reflected by the existence of branches in their X-ray colour–colour diagrams), and correlated QPO behaviour. After early attempts to classify QPO sources (Stella 1986) it was suggested by Priedhorsky *et al.* (1986), van der Klis *et al.*

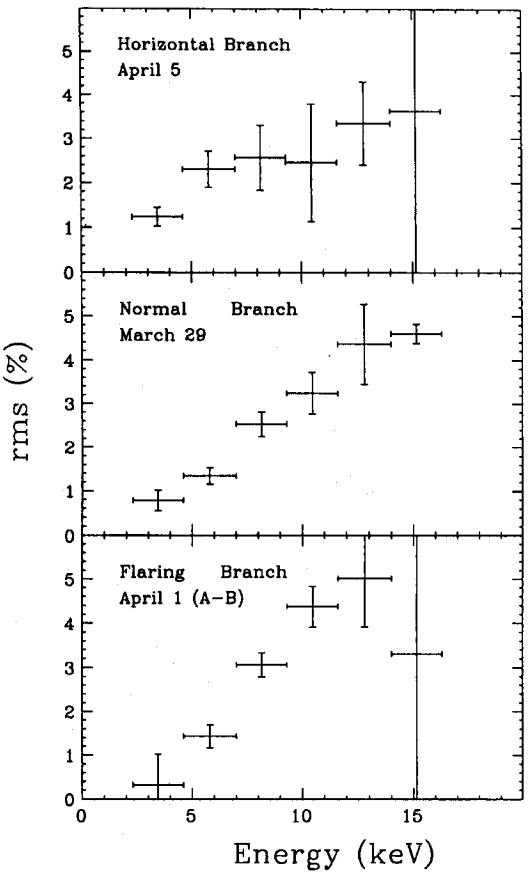

Figure 6. Representative energy spectra of QPO on the horizontal (April 5), normal (March 29) and flaring branch (April 1; A–B, see Table 2).

Table 4. Energy dependence of QPO rms modulation (%).

MPC-3 data	March 29	March 31	April 1 (A-B)	April 1 (C-F)	April 1 (G)	April 4	April 5
	NB	NB	FB	NB	FB	HB	HB
Freq (Hz)	7.4	6.8	13.5	7.0	18.9	26.0	21.0
FWHM (Hz)	5.5	1.6	6.0	1.9	6.1	4.5	6.8
1-2.3 keV	0.07±0.20	0.03±0.31	1.31±0.73	0.52±0.29	1.21±0.72	1.12±0.41	1.47±0.22
2.3-4.6 keV	0.78±0.23	0.30±0.37	0.32±0.70	0.29±0.18	0.63±0.37	1.05±0.32	1.24±0.21
4.6-7.0 keV	1.34±0.19	0.69±0.27	1.43±0.26	0.65±0.14	0.99±0.33	1.78±0.46	2.30±0.41
7.0-9.3 keV	2.53±0.28	1.66±0.27	3.06±0.27	1.31±0.18	1.61±0.45	1.93±0.98	2.57±0.74
9.3-11.6 keV	3.24±0.48	1.75±0.70	4.37±0.46	1.77±0.31	1.64±1.14	3.25±0.96	2.46±1.33
11.6-14.0 keV	4.36±0.91	3.43±0.78	5.01±1.10	0.23±0.82	0.43±1.63	2.64±1.32	3.35±0.95
14.0-16.3 keV	4.60±1.21	3.91±2.33	3.30±5.14	0.39±1.73	0.75±2.15	3.47±1.41	3.63±3.69

(1987) and Hasinger (1987a) that the QPO properties of LMXB are correlated with the X-ray spectrum as indicated by the location of the spectral state in an X-ray hardness–intensity diagram.

It now appears from a recent survey (Hasinger & van der Klis 1989) of the fast variability characteristics of LMXB and their relation to X-ray spectral properties that the LMXB can be divided in two groups; one group contains the 'Z sources' and the other the 'atoll sources'.

The Z sources, as first recognized by Hasinger (1987b, 1988), are characterized by three branches in an X-ray colour–colour diagram, the horizontal branch, the normal branch and the flaring branch, which are arranged in a Z-like pattern (GX 17+2 is a Z source). The frequency of the QPO in the horizontal branch varies beween ~20 and ~50 Hz, and is positively correlated with the source intensity. In the normal branch the QPO frequency does not vary much with source intensity; typical values for different sources range between ~5 to ~7 Hz. In the flaring branch the QPO frequency is positively correlated with source intensity (the latter form of QPO has only been observed in the Z source Sco X-1 before this work).

The atoll sources show a different X-ray colour–colour diagram, in which a 'banana shaped' branch (with a positive correlation of hardness and intensity), and isolated 'islands' can be distinguished. The atoll sources, in general, do not show QPO of the kinds observed in the Z sources; their power spectra often do show wiggles, bumps and broad peaks, on top of very broad noise components (which can extend all the way to ~100 Hz).

The results that we have obtained from our *Ginga* observations of GX 17+2 have led to the discovery of flaring branch QPO from this source, and confirm the earlier conclusion, based on *EXOSAT* results (Stella *et al.* 1987; Langmeier *et al.* 1989) that GX 17+2 belongs to the group of Z sources. This indicates that the (correlated) spectral and temporal properties of bright LMXB, as described above, do not change over time-scales of years. This stability in the properties of GX 17+2 can be expressed in a quantitative way, by noting that the average frequencies of the normal-branch QPO, as observed with *EXOSAT* (7.2±0.2 Hz, Stella *et al.* 1987) and with *Ginga* (7.1±0.1 Hz, see Table 2), are the same to within the accuracy of their determination. The same result was obtained for Cyg X-2 (Hasinger 1987a; Norris & Wood 1987).

During our observations, GX 17+2 showed a broad peak in the power spectrum at frequencies above $\sim 10^2$ Hz when it was in the flaring branch spectral state; (it then also showed QPO beween 7 and 20 Hz). A peak at very high frequencies had previously been reported only from Cir X-1 (Tennant 1987). Also Cir X-1 then simultaneously showed QPO at 5–20 Hz. Both in Cir X-1 and in GX 17+2, the high-frequency peak is consistent with having a relative width (FWHM/ν_c) of up to 0.7, and therefore it may be similar to the 'peaked high-frequency noise (HFN)' sometimes seen in atoll sources (Hasinger & van der Klis 1989). A further similarity between the timing behaviour of Cir X-1 and GX 17+2 is that in both sources the spectral branch in a hardness–intensity diagram, in which these simultaneous 10–20 Hz QPO and $>10^2$ Hz broad peaks were seen, is connected with another spectral branch in which QPO are observed at ~6 Hz (independent of the source intensity). In GX 17+2 the latter spectral branch is, of course, the normal branch. This similarity between Cir X-1 and GX 17+2 suggests that the spectral branches found by Tennant (1987, 1988) can perhaps be identified with the normal and flaring branches. Cir X-1 may therefore be a Z source (*cf.* Lewin *et al.* 1988).

The physics behind the X-ray branches is not well understood. In view of the discontinuity in the QPO and LFN properties at the apex where the horizontal and normal branches are linked, it is now generally believed that horizontal branch QPO and normal branch QPO are caused by different physical mechanisms (Hasinger 1987b; Lamb 1989; van der Klis 1989b). Our observations of GX 17+2, and those of Sco X-1 (Priedhorsky *et al.* 1986), and possibly Cir X-1 (Tennant 1987, 1988), show that the QPO properties change smoothly as the source moves from the normal branch on to the flaring branch. This continuity in the QPO behaviour indicates that the normal-branch QPO and the flaring branch QPO are likely to be one single physical phenomenon.

It seems likely that the parameter that determines the position of the source in the Z track is the mass accretion rate. Recent simultaneous X-ray (Hasinger *et al.* 1989b), UV (Vrtilek *et al.* 1990) and optical (van Paradijs *et al.* 1990) observations strongly suggest that the accretion rate increases as a source moves from the horizontal branch via the normal branch to the flaring branch. We briefly discuss how this result fits the main models proposed for the QPO.

If the magnetospheric beat-frequency model (Alpar & Shaham 1985) explains the horizontal-branch QPO, the mass accretion rate must *increase* as the source moves to the right on the horizontal branch, toward the normal branch.

In the context of the 'flywheel' scenario for Sco X-1, in which the rotational energy of the neutron star is used as a source of X-ray luminosity when the source is in the normal branch, Priedhorsky (1986) also suggested that the mass accretion rate *increases* as the source moves from the horizontal branch, down the normal branch, to the far right on the flaring branch. According to this scenario the total luminosity would reach a minimum value of $\sim 10^{36-37}$ erg s^{-1} at the transition from the flaring branch to the 'quiescent' (=normal) branch. The flaring branch and the normal branch can be described with this scenario; however, the horizontal branch in Sco X-1, which was not known at the time Priedhorsky made his suggestion, is difficult to explain. Hasinger *et al.* (1989a) pointed out that the above scenario may not be tenable, because the transition from the flaring branch to the normal branch in Cyg X-2 occurs at $\sim 10^{38}$ erg s^{-1}.

Van der Klis *et al.* (1987) speculate on an occultation scenario (suggested for Sco X-1) whereby the accretion rate *decreases* as the source moves from the normal branch to the flaring branch (at the time of their suggestion the horizontal branch in Sco X-1 was not known yet). In this model the (NB and FB) QPO are explained in terms of occultations at the Kepler frequency corresponding to the radius of the radiation-pressure dominated inner part of the disc. This model can explain the presence of the NB–FB QPO and the increase of the QPO frequency from the NB to the FB, but not the high-frequency QPO in the HB.

Hasinger (1987b) suggested that the luminosity of normal-branch QPO sources is near the Eddington limit and that the

~6-Hz QPO are associated with a radiation-dominated accretion flow. To explain the remarkable stability of their frequency he noted that near the Eddington limit the effective gravity is strongly reduced, and that the relevant propagation speed of disturbances may then be the speed of sound. From a thermalization argument, Hasinger (1987b) inferred that the frequency (ν_f) given by the ratio of sound speed to the circumference of the neutron star depends only very weakly on the accretion rate, and is approximately that observed for normal-branch QPO. A more detailed model of instabilities in a radiation-dominated accretion flow was recently proposed by Lamb (1989). In this model, at a near-Eddington accretion luminosity, the inflow from a spherical corona of radius $\sim 10^7$ cm reacts (negatively) to fluctuations in the luminosity on a time-scale determined by the size of the corona and the sound speed.

In the beat-frequency mode (Alpar & Shaham 1985), which is often used to describe the horizontal branch QPO, the FWHM is determined by the lifetime of the shots. One would thus, to first approximation, expect that the FWHM of the first and second harmonic would have the same FWHM (in units of Hz). In contrast, if QPO are produced by a slowly changing frequency, as was observed for the 6-Hz QPO in the Rapid Burster (Dotani *et al.* 1989), we would expect a FWHM ratio of the second and first harmonic of 2. The ratio of the two FWHM in first and second harmonic, as was found for the horizontal branch in this data set, was 2.02 ± 0.46 (90 per cent error bar), favouring a model in which the QPO are produced by a slowly changing frequency.

In the above models (Hasinger 1987b; Lamb 1989) the mass-transfer rate increases monotonically as the spectral state changes from the horizontal branch, via the normal branch to the flaring branch. The spectral transitions correspond to critical mass transfer rates, whereby at the lowest point of the normal branch the Eddington limit is reached, and the mass transfer becomes super-Eddington (possibly accompanied by the ejection of matter) on the flaring branch.

According to this picture, all Z sources with a normal and flaring branch must radiate, during a fair fraction of their time, at or near the Eddington limit. [We note that in the case of Sco X-1 this would imply that the distance is of the order of 2 kpc, unless the X-rays from Sco X-1 are emitted highly anisotropically. This may be hard to reconcile with the recent determination of 250 pc for the distance of Sco X-1 (Knude 1987).] Evolutionary arguments (see e.g. Pylyser & Savonije 1988, and references therein) indicate that there is no reason why the mass-transfer rate of low-mass X-ray binaries should not be larger than the value corresponding to the Eddington limit.

Variations in the mass-transfer rate of sub-Eddington sources (whose X-ray luminosities range from $\sim 10^{-3}$–0.3 L_{Edd}, e.g. burst sources, see van Paradijs *et al.* 1979), as inferred from the variations of their X-ray fluxes, are generally rather large (factors of ~10, Forman *et al.* 1978). If the same were the case for Z sources, whose intensities vary only by a factor of $\lesssim 3$ (Forman *et al.* 1978), we have to conclude that their apparent intensity variations do not fully reflect variations in mass-transfer rate. It is well possible that during the flaring branch the accretion rates are substantially above the Eddington limit, yet the source keeps emitting X-rays near the Eddington intensity. [The super-Eddington part could e.g. be transformed into kinetic energy of a jet. It is of interest to note in this connection that some LMXB have double lobed radio jets (e.g. Sco X-1 and Cyg X-3, see Geldzahler & Fomalont 1986; Strom, van Paradijs & van der Klis 1989), which may be related to super-Eddington accretion.]

5 CONCLUSION

Our *Ginga* observations confirm that GX 17+2 is a typical Z source. It shows the horizontal, normal and flaring branches in the X-ray colour–colour diagram, with correlated fast variability behaviour. When GX 17+2 is in the horizontal branch it shows QPO (and associated LFN) whose frequency (~20–30 Hz) increases as the source moves toward the normal branch. The relative widths of the first and second harmonic of the HB QPO peaks are inconsistent with pure lifetime broadening but suggest, instead, frequency variations as the broadening mechanism. On the normal branch the QPO have a fixed frequency, which is independent of the source intensity; the average normal-branch QPO frequency appears not to vary over time-scales of years. When GX 17+2 moves from the normal to the flaring branch the QPO frequency increases. This behaviour is very similar to that observed for Sco X-1, the only source in which flaring branch QPO were previously observed.

ACKNOWLEDGMENTS

We thank the *Ginga* team for executing the X-ray observations. WP and WHGL thank Professors Makino and Tanaka at ISAS for their hospitality. We thank Dr T. Dotani for assistance in the data-analysis. We thank Dr G. Hasinger for many useful suggestions. AAZ acknowledges support from The Netherlands Foundation of Astronomical Research (ASTRON) with financial aid from the Netherlands Organization for Scientific Research (NWO). WP received support from NWO and the ministry of Education and Sciences. JvP acknowledges support from NATO under grant RG 0331/88. WHGL ackowledges support from the United States National Aeronautics and Space Administration under grants NAG8-674, NSG-7643 and NAG8-700, and from NWO.

REFERENCES

Alpar, M. A. & Shaham, J., 1985, *Nature*, **316**, 239.
Avni, Y. 1976. *Astrophys. J.*, **210**, 642.
Bradt, H. V., Burnett, B., Mayer, W., Rappaport, S. & Schnopper, H., 1971. *Nature*, **229**, 96.
Davidsen, A., Malina, A. & Bowyer, S., 1976. *Astrophys. J.*, **203**, 448.
Dotani, T., Mitsuda, K., Inoue, H., Tanaka, Y., Kawai, N., Tawara, Y., Makishima, K., van Paradijs, J., Penninx, W., van der Klis, M., Tan, J. & Lewin, W., 1989. *Astrophys. J.*, in press.
Forman, W., Jones, C. & Tananbaum, H., 1976. *Astrophys. J.*, **208**, 849.
Forman, W., Jones, C., Cominsky, P., Julien, P., Murray, S., Peters, G., Tananbaum, H. & Giacconi, R., 1978. *Astrophys. J. Suppl.*, **38**, 357.
Garcia, M. R., 1987. *PhD thesis*, Harvard University, Cambridge, U.S.A.

Geldzahler, B. J. & Fomalont, E. B., 1986. *Astrophys. J.*, **311,** 805.
Grindlay, J. E. & Seaquist, E. R., 1986. *Astrophys. J.*, **310,** 172.
Hasinger, G., 1987a. In: *The Origin and Evolution of Neutron Stars, IAU Symp. No. 125,* p. 333, eds Helfand, D. J. & Huang, J.-H, Reidel, Dordrecht.
Hasinger, G., 1987b, *Astr. Astrophys.*, **186,** 153.
Hasinger, G., 1988. In: *Physics of Neutron Stars and Black Holes,* p. 97, ed. Tanaka, Y., Universal Academy Press.
Hasinger, G. & van der Klis, M., 1989. *Astr. Astrophys.*, **225,** 79.
Hasinger, G., Middleditch, J. & Priedhorsky, W. C., 1989a. *Astrophys. J.*, **337,** 843.
Hasinger, G., van der Klis, M., Mitsuda, K., Dotani, T. & Ebisawa, A., 1989b. *Astrophys. J.*, submitted.
Hertz, P. & Wood, K. S. 1986. In: *Variability of Galactic and Extragalactic X-ray Sources,* p. 221, Associazone per l'Avanzamento dell' Astronomia, ed. Treves, A., Milano-Bologna.
Hjellming, R. M. & Wade, C. M., 1971. *Astrophys. J.*, **168,** L21.
Kahn, S. M. & Grindlay, J. E., 1984. *Astrophys. J.*, **281,** 826.
Knude, J., 1987. *Astr. Astrophys.*, **171,** 289.
Lamb, F. K., 1989. *Astrophys. J.*, in press.
Langmeier, A., Hasinger, G. & Trümper, J., 1990. *Astr. Astrophys.*, in press.
Langmeier, A., Hasinger, G., Sztajno, M., Trümper, J. & Pietsch, W., 1985. *IAU Circ. No. 4147.*
Langmeier, A., Sztajno, M., Vacca, W. D., Trümper, J. & Pietsch, W., 1986. In: *The Evolution of Galactic X-ray Binaries,* NATO ASI Series C, p. 253, eds Trümper, J., Lewin, W. H. G. & Brinkmann, W., D. Reidel, Dordrecht.
Lewin, W. H. G. & van Paradijs, J., 1985. *Astro. Astrophys.*, **142,** 361.
Lewin, W. H. G., van Paradijs, J. & van der Klis, M., 1988. *Space Sci. Rev.*, **46,** 273.
McHardy, I. M., Lawrence, A., Pye, J. P. & Pounds, K. A., 1981. *Mon. Not. R. astr. Soc.*, **197,** 893.
Makino, M. & *GINGA* team, 1987. *Astrophys. Lett.*, **25,** 223.
Middleditch, J. & Priedhorsky, W. C., 1986. *Astrophys. J.*, **306,** 230.
Mitsuda, K. & Dotani, T., 1989a. *Publs astr. Soc. Japan,* **41,** 557.
Mitsuda, K. & Dotani, T., 1989b. *Publs astr. Soc. Japan,* in press.
Norris, J. P. & Wood, K. S., 1987. *Astrophys. J.*, **312,** 732.
Penninx, W., Lewin, W. H. G., Zijlstra, A. A., Mitsuda, K., van Paradijs, J. & van der Klis, M., 1988. *Nature,* **336,** 146.
Penninx, W. *et al.,* 1989. In preparation.
Ponman, T., 1982a. *Mon. Not. R. astr. Soc.*, **200,** 351.
Ponman, T. 1982b. *Mon. Not. R. astr. Soc.*, **201,** 769.
Priedhorsky, W., 1986. *Astrophys. J.*, **306,** L97.
Priedhorsky, W., Hasinger, G., Lewin, W. H. G., Middleditch, J., Parma, A., Stella, L. & White, N., 1986. *Astrophys. J.*, **306,** L91.
Pylyser, E. & Savonije, G. J., 1988. *Astr. Astrophys.*, **191,** 57.
Stella, L., 1986. In: *Plasma Penetration into Magnetospheres,* p. 199, eds Kylafis, N., Papamastorakis, J. & Ventura, J., Crete University Press, Iraklion.
Stella, L., Parmar, A. N. & White, N. E., 1987. *Astrophys. J.*, **321,** 418.
Strom, R. G., van Paradijs, J. & van der Klis, M., 1989. *Nature,* **337,** 234.
Sztajno, M., van Paradijs, J., Lewin, W. H. G., Langmeier, A., Trümper, J. & Pietsch, W., 1986. *Mon. Not. R. astr. Soc.*, **222,** 499.
Tarenghi, M. & Reina, C., 1972. *Nature Phys. Sci.*, **240,** 53.
Tawara, Y., Hirano, T., Kii, T., Matsuoka, M. & Murakami, T., 1984. *Publs astr. Soc. Japan,* **36,** 861.
Tennant, A. C., 1987. *Mon. Not. R. astr. Soc.*, **226,** 971.
Tennant, A. C., 1988. *Mon. Not. R. astr. Soc.*, **230,** 403.
Turner, M. J. L. *et al.*, 1989. *Publs astr. Soc. Japan,* **41,** 345.
van der Klis, M., 1989a. *In: Timing Neutron Stars,* eds Ögelman, H. & van den Heuvel, E. P. J., Kluwer, Dordrecht
van der Klis, M., 1989b. *Ann. Rev. astr. Astrophys.*, **27,** 517.
van der Klis, M., Jansen, F., van Paradijs, J., Lewin, W. H. G., van den Heuvel, E., Trümper, J. & Sztajno, M., 1985. *Nature,* **231,** 379.
van der Klis, M., Stella, L., White, N., Jansen, F. & Parmar, A. N., 1987. *Astrophys. J.*, **316,** 411.
van Paradijs, J., Joss, P. C., Cominsky, L. & Lewin, W. H. G., 1979. *Nature,* **280,** 377.
van Paradijs, J., Penninx, W. & Lewin, W. H. G., 1988. *Mon. Not. R. astr. Soc.*, **233,** 437.
van Paradijs, J., Allington-Smith, J., Callanan, P., Charles, P. A., Hassall, B. J. M., Machin, G., Mason, K. O., Naylor, T. & Smale, A. P., 1990. *Astr. Astrophys.*, submitted.
Vaughan, B. *et al.*, 1989. *Astrophys. J.*, to be submitted.
Vrtilek, S., Raymond, J., Garcia, M. R., Verbunt, F., Hasinger, G. & Kürster, M., 1990. *Astr. Astrophys.*, in press.
White, N. E., Mason, K. O., Huckle, H. E., Charles, P. A. & Stanford, P. W., 1976, *Astrophys. J.*, **209,** L119.
White, N. E., Mason, K. O., Sanford, P. W., Johnson, H. M. & Catura, R. C., 1978. *Astrophys. J.*, **220,** 600.